

# ***Meta* and *para*-Xylene Oxidation: Experimental Results in a JSR, Comprehensive Kinetic Modeling**

S. Gaïl, P. Dagaut\*

Laboratoire de Combustion et Systèmes Réactifs,  
1C, Avenue de la Recherche-Scientifique,  
45071 Orléans cedex 2, France

## **Abstract**

The oxidation of *meta* and *para*-xylene were studied in a jet-stirred reactor at atmospheric pressure. New experimental results were obtained over the high temperature range 1050-1400K, and variable equivalence ratio ( $0.5 \leq \phi \leq 1.5$ ). The oxidation of *meta* and *para*-xylene in these conditions were modeled using a detailed kinetic reaction mechanism (189 species and 1359 reactions, most of them reversible).

## **Introduction**

Aromatic hydrocarbons like xylenes represent an important fraction of commercial gasoline (c.a. 14% in wt.), and are also present in Diesel fuel and kerosene [1]. Nevertheless, the oxidation and pyrolysis of aromatic hydrocarbons are far from being understood [2]. In order to reduce the emission of pollutants and toxic compounds, detailed modeling of combustion in engines is undertaken by engine makers. However, due to the high complexity of commercial fuels, these models need kinetic reaction mechanisms for the combustion of simple surrogate fuels including representative hydrocarbons [3,4]. Benzene and toluene have been studied extensively and kinetic models were proposed [5-7]. However, these fuels are not complex enough to represent the aromatics present in kerosene and Diesel fuels. N-propyl-benzene, which is present in commercial gasoline, Diesel fuel, and kerosene [1], could be included in the corresponding model fuels [7,8]. Xylenes are also good candidates to represent the poly-substituted aromatic fraction of commercial fuels such as gasoline.

Several years ago, Emdee *et al.* [9] proposed a reaction scheme for the oxidation of *m*- and *p*-xylene based on atmospheric flow reactor experiments performed over the temperature range 1093 to 1199 K and for equivalence ratio ranging from 0.47 to 1.7. Gregory *et al.* [10] investigated the chemistry leading to the formation, in engines exhaust, of aromatic hydrocarbons from deuterium-labeled isomeric xylenes. Roubaud *et al.* [11] also studied the auto-ignition delays of xylenes in a rapid compression machine in the low-temperature oxidation regime ( $5 < P / \text{bar} < 25$ , 600-900 K). Dupont [12] studied the combustion of a methane flat flame seeded with *p*-xylene under low-pressure conditions.

In the present work, the oxidation of *m*- and *p*-xylene was investigated experimentally over a wide range of conditions (1050-1400 K at 1 atm /  $10^5$  Pa and  $\Phi=0.5$  to 1.5) using a fused-silica jet-stirred reactor (JSR). Concentration profiles of reactants, stable intermediates and final products were measured by low pressure sonic probe sampling followed by on-line and off-line gas

chromatography analyses (GC-FID/TCD/MS). These results were interpreted in terms of a detailed chemical kinetic reaction mechanism.

## **Experimental set up**

The JSR experiment used in this work is similar to that described earlier [13,14]. The reactor consisted of a small sphere of 40 mm diameter ( $30.5 \text{ cm}^3$ ) made of fused silica (to minimize wall catalytic reactions), equipped with 4 nozzles of 1 mm I.D. for the admission of the gases which achieve the stirring. A nitrogen flow of 100 L/h was used to dilute the fuel and avoid its pyrolysis before admission in the reactor. All the gases were preheated before injection in order to minimize temperature gradients inside the JSR. The reactants were diluted by nitrogen ( $<50$  ppm of  $\text{O}_2$ ;  $<1000$  ppm of Ar;  $<5$  ppm of  $\text{H}_2$ ), and mixed at the entrance of the injectors [13]. High purity reactants were used in these experiments: oxygen was 99.995% pure and xylenes  $>99\%$  pure. Furthermore, xylenes were sonically degassed before use. A piston pump (Shimadzu LC-10AD VP) was used to deliver the fuel to an atomizer-vaporizer assembly maintained at  $120^\circ\text{C}$ . A good thermal homogeneity along the whole vertical axis of the reactor was observed for each experiment by thermocouple (0.1 mm Pt-Pt/Rh 10% located inside a thin-wall silica tube) measurements (temperature change  $\leq 5$  K). The reacting mixtures were sampled via a low-pressure fused-silica sonic probe. The samples (30 Torr / 4 kPa) were taken at steady temperature and residence time. They were analyzed on-line by a GC-MS or FID and off-line after collection and storage in 1 L Pyrex bulbs: Low vapor-pressure compounds were analyzed on-line whereas permanent gases and high vapor-pressure species were analyzed off-line. All the products were analyzed by a chromatographic peak identified. The detection of aromatics (benzene, toluene, *m*- and *p*-xylene) from the on-line and off-line analyses was used to calibrate the measurements performed on-line. These species were used as internal standards in the on-line analyses whereas relative response coefficients were derived from the injection of pure

---

\* Corresponding author: dagaut@cnrs-orleans.fr

compounds (external standards) on both analytical systems. The present experiments were performed at steady state, at a constant mean residence time of 0.1 s, the reactants flowing continually in the reactor, varying stepwise the temperature of the gases inside the JSR. A high degree of dilution (0.1% vol. of fuel) was used, reducing temperature gradients in the JSR and heat release (no flame occurred in the JSR).

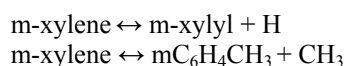
Several gas chromatographs (GC), equipped with capillary columns (Poraplot-U, Molecular Sieve-5A, DB-5ms, DB-624, Plot Al<sub>2</sub>O<sub>3</sub>/KCl, Carboplot-P7), thermal conductivity detector (TCD) and flame ionization detector (FID), were used for stable species measurements. Compound identifications were made through GC/MS analyses of the samples. Ion trap detectors operating in electron impact ionization mode (GC/MS Varian Saturn 3) were used. CH<sub>2</sub>O and CO<sub>2</sub> were measured by FID after hydrogenation on a methanizer (Ni/H<sub>2</sub> catalyst) connected to the exit of the Poraplot-U GC column. A good repeatability of the measurements and a reasonably good carbon balance (100±10%) were obtained in this series of experiments.

### Kinetic modeling

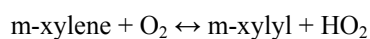
The JSR modeling was performed using the PSR computer code [15] that computes species concentrations from the balance between the net rate of production of each species by chemical reaction and the difference between the input and output flow rates of species. The reaction mechanism used in this study is based on a comprehensive mechanism developed for the oxidation of natural gas blends to diesel fuel [5]. The reaction mechanism used here consisted of 1359 reversible reactions involving 189 species. It has a strong hierarchical structure. Since most of the present mechanism has been presented in detail in previous papers [6-8, 16-20], only the reaction sub-mechanism for the oxidation of *m*- and *p*-xylene is presented here. The rates of reaction were computed from the kinetic reaction mechanism and the rate constants of the elementary reactions calculated at the experimental temperature, using the modified Arrhenius equation,  $k = A \times T^b \times \exp(-E/RT)$ . The rate constants for the reverse reactions were computed from the forward rate constants and the equilibrium constants ( $K_c = k_{\text{forward}} / k_{\text{reverse}}$ ) calculated using the appropriate thermochemical data [21-24]. The pressure dependencies of the unimolecular reactions and of some pressure-dependent bimolecular reactions were taken into account when information was available (i.e.,  $k(P,T)$ ). First-order local sensitivity analyses and reaction rates analyses were performed computing rates of consumption (ROC) and production (ROP) for every species. The present scheme was also used to successfully simulate the oxidation of benzene and toluene in conditions similar to those of the present study, as well as their ignition delays and flame speeds in air [5-8]. Figures 1 to 8 compare the modeling results obtained for the oxidation of *m*- and *p*-xylene in a JSR, using the presently proposed scheme.

In the proposed mechanism, *m*- and *p*-xylene oxidation have the same structure. However, in this work, a difference between *m*- and *p*-xylene oxidation is highlighted. It concerns the simultaneous and the sequential oxidation of the methyl groups for *p*-xylene and *m*-xylene respectively. In this part, we describe only the sub-mechanism for *m*-xylene. The part concerning the simultaneous oxidation of *p*-xylene, not included for *m*-xylene, is also described.

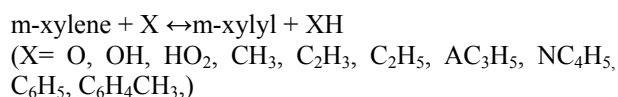
The initiation reactions for the oxidation of *m*-xylene include two thermal decomposition, one yielding *m*-methyl-benzyl (*m*-xylyl) and H-atom, and the other one producing *m*-methyl-phenyl (mC<sub>6</sub>H<sub>4</sub>CH<sub>3</sub>) and CH<sub>3</sub>.



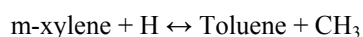
Initiation also occurs by reaction with molecular oxygen. It yields the *m*-methyl-benzyl radical and HO<sub>2</sub>.



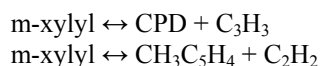
Propagation reactions proceed via H-atom abstraction by atoms and radicals yielding *m*-methyl-benzyl:



The kinetics of these reactions were estimated based on [6,25]. Displacement reaction of the methyl group by a H-atom, by analogy with the displacement reaction of toluene, yields toluene and methyl. The kinetics was assumed based on that of toluene + H ↔ benzene + CH<sub>3</sub> [26].



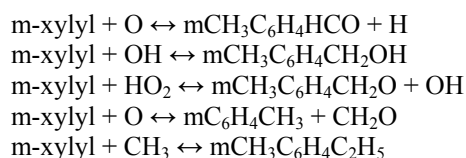
The *m*-methyl-benzyl radical (*m*-xylyl) reacts by thermal decomposition yielding acetylene and methyl-cyclopentadienyl (CH<sub>3</sub>C<sub>5</sub>H<sub>4</sub>), the propargyl radical (C<sub>3</sub>H<sub>3</sub>) and 1,3-cyclopentadiene (CPD).



In the case of *p*-xylene there is a third thermal decomposition yielding the *p*-xylylene (pCH<sub>2</sub>C<sub>6</sub>H<sub>4</sub>CH<sub>2</sub>) or *p*-quinodimethane (3,6-bis(methylene)-1,4-cyclohexadiene).

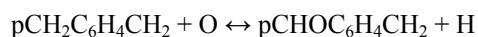
Reactions of *m*-methyl-benzyl with molecular oxygen, O, OH, CH<sub>3</sub> and HO<sub>2</sub> produce, *m*-methyl-benzaldehyde (mCH<sub>3</sub>C<sub>6</sub>H<sub>4</sub>HCO), *m*-methyl-benzyl alcohol (mCH<sub>3</sub>C<sub>6</sub>H<sub>4</sub>-CH<sub>2</sub>OH), *m*-methyl-benzyloxy radical (mCH<sub>3</sub>C<sub>6</sub>H<sub>4</sub>CH<sub>2</sub>O), *m*-methyl-phenyl, *m*-methyl-ethylbenzene (mCH<sub>3</sub>C<sub>6</sub>H<sub>4</sub>C<sub>2</sub>H<sub>5</sub>) and formaldehyde:



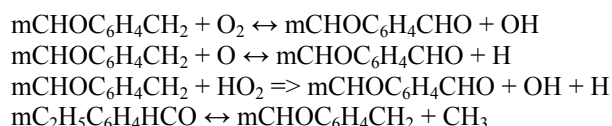


*M*-methyl-benzaldehyde reacts by thermal decomposition yielding a benzylic radical, with an aldehyde group ( $m\text{CHOC}_6\text{H}_4\text{CH}_2$ ), and a H-atom.

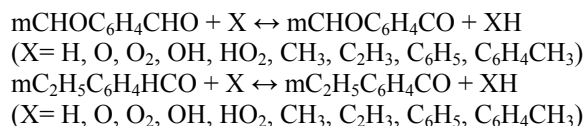
In the case of *p*-xylene, *p*-xylylene reacts through addition of O-atom to the double bond forming also a benzylic radical with an aldehyde group ( $p\text{CHOC}_6\text{H}_4\text{CH}_2$ ).



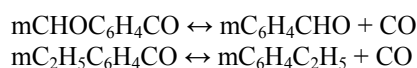
This benzylic radical then reacts similarly to the methylbenzyl radical and the  $m\text{CHOC}_6\text{H}_4\text{CH}_2$  radical to form *m*-phthalaldehyde ( $m\text{CHOC}_6\text{H}_4\text{CHO}$ ) or *m*-ethylbenzaldehyde ( $m\text{C}_2\text{H}_5\text{C}_6\text{H}_4\text{HCO}$ ):



These aldehydes are consumed mainly through abstraction of an aldehydic H-atom to form benzylic radicals:

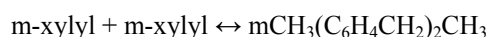


The benzylic radical then decomposes to phenylic radicals and CO:



In this model, the fate of the phenylic radical is either through further oxidation to form phenoxy type radicals or formation of stable species through H-atom abstraction from a stable hydrocarbon.

Finally, the recombination of methylbenzyl yields 3,3'-dimethylbibenzyl ( $m\text{CH}_3(\text{C}_6\text{H}_4\text{CH}_2)_2\text{CH}_3$ ); its kinetics was taken from [27].



## Results and Discussion

### *m*-Xylene Oxidation in a JSR at 1 atm

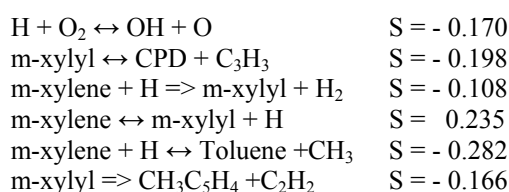
Molecular species concentration profiles were obtained from the oxidation of *m*-xylene in a JSR: O<sub>2</sub>, CO, CO<sub>2</sub>, CH<sub>2</sub>O, CH<sub>4</sub>, C<sub>2</sub>H<sub>2</sub>, C<sub>2</sub>H<sub>4</sub>, C<sub>2</sub>H<sub>6</sub>, allene (AC<sub>3</sub>H<sub>4</sub>), propyne (PC<sub>3</sub>H<sub>4</sub>), C<sub>3</sub>H<sub>6</sub>, acrolein, 1,3-C<sub>4</sub>H<sub>6</sub>, vinylacetylene, 1,3-cyclopentadiene, benzaldehyde, phenol, benzene,

styrene, phenol, toluene, ethylbenzene, methyl-ethylbenzene, *p*-methyl-benzaldehyde, phthalaldehyde, ethylbenzaldehyde, methylstyrene, *o*-xylene, cresols, naphthalene, dibenzyl, and 3,3'-dimethylbibenzyl were measured by sonic probe sampling and GC analyses. The products detected here and their relative abundances are in line with the experimental results obtained in a previous plug-flow reactor study [9], although acrolein, phenol and dibenzyl were not reported in that previous work.

Figures 1 to 4 present the results obtained at 1 atm for  $\Phi=1.0$ . The initial conditions were: *m*-xylene, 0.1%; O<sub>2</sub>, 1.05%, N<sub>2</sub>, 98.85%,  $\tau=0.1\text{s}$ ;  $\phi=1.0$ .

The experimental results show that besides CO, H<sub>2</sub>, and CO<sub>2</sub>, the major intermediate products were acetylene (C<sub>2</sub>H<sub>2</sub>), methane (CH<sub>4</sub>), toluene, benzene, styrene, formaldehyde (CH<sub>2</sub>O), 1,3-cyclopentadiene (CPD), *m*-methyl-benzaldehyde, ethylene (C<sub>2</sub>H<sub>4</sub>), vinylacetylene (C<sub>4</sub>H<sub>4</sub>) and propyne. The minor products were benzaldehyde, ethane, allene, acrolein, dibenzyl, formaldehyde, ethylbenzene, *m*-methylstyrene, *m*-methyl-ethylbenzene, naphthalene and 3,3'-dimethylbibenzyl. Only trace amounts of *o*-xylene, indene, methyl-naphthalene, anthracene, phenanthrene, phenylacetylene, ethyl-benzaldehyde, and methyl-biphenyl were detected; they are not shown here.

Sensitivity analyses and reaction path analyses, based on species reaction rate of production and rate of consumption computations, were used to elaborate the presently proposed mechanism and interpret the results. According to these computations, the kinetics of *m*-xylene oxidation in the present experimental conditions is mainly sensitive to a limited number of reactions pertaining to its oxidation sub-mechanism and to reactions of simple intermediates. At 1300K, in stoichiometric conditions and at 1 atm, *m*-xylylene computed mole fractions are mostly sensitive to:



### *p*-Xylene Oxidation in a JSR at 1 atm

From the oxidation of *p*-xylene, molecular species concentration profiles were obtained for H<sub>2</sub>, O<sub>2</sub>, CO, CO<sub>2</sub>, CH<sub>2</sub>O, CH<sub>4</sub>, C<sub>2</sub>H<sub>2</sub>, C<sub>2</sub>H<sub>4</sub>, C<sub>2</sub>H<sub>6</sub>, C<sub>3</sub>H<sub>4</sub> (allene and propyne), C<sub>3</sub>H<sub>6</sub>, 1,3-C<sub>4</sub>H<sub>6</sub>, vinylacetylene, cyclopentadiene, benzaldehyde, phenol, benzene, styrene, toluene, ethylbenzene, methyl-ethylbenzene, methylbenzaldehyde, phthalaldehyde, ethylbenzaldehyde, methylstyrene, *o*-xylene, cresols, naphthalene and 4,4'-dimethylbibenzyl by probe sampling and GC analysis. The products detected here are in agreement with the experimental results obtained in previous plug-flow reactor studies [10], although acrolein, phenol dibenzyl and cresols were not reported there.

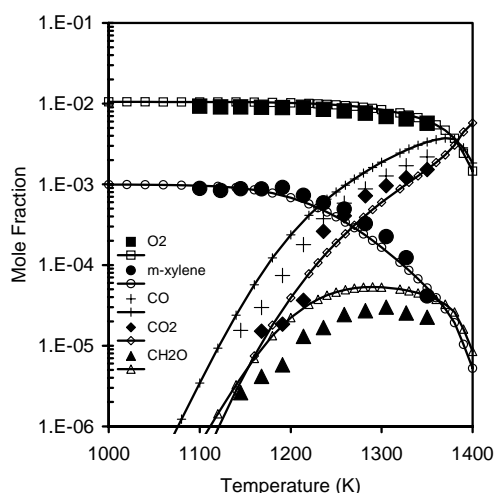


Fig. 1. *M*-xylene oxidation in a JSR at 1 atm. Experimental data (symbols) for CO, formaldehyde ( $\text{CH}_2\text{O}$ ), oxygen and *m*-xylene are compared to computations

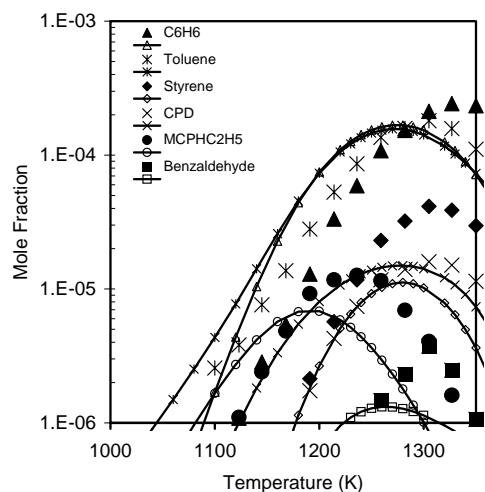


Fig. 2. *M*-xylene oxidation in a JSR at 1 atm. Experimental data (symbols) for benzene ( $\text{C}_6\text{H}_6$ ), toluene, styrene, cyclopentadiene (CPD), *m*-methyl-ethylbenzene (MCPHC2H5), benzaldehyde are compared to computations

The present data were used to propose a detailed kinetic reaction mechanism for the oxidation of *p*-xylene. Figures 4 to 8 present the results obtained at 1 atm for  $\phi=1.0$ . The experimental results show that besides  $\text{CO}$ ,  $\text{H}_2$ , and  $\text{CO}_2$ , the major intermediate products are acetylene ( $\text{C}_2\text{H}_2$ ), methane ( $\text{CH}_4$ ), toluene, benzene, styrene, formaldehyde ( $\text{CH}_2\text{O}$ ), cyclopentadiene (CPD), *p*-phthalaldehyde, *p*-methyl-benzaldehyde (pMeBAL), ethylene ( $\text{C}_2\text{H}_4$ ), vinylacetylene ( $\text{C}_4\text{H}_4$ ) and propyne. The minor products are benzaldehyde, ethane, allene, acrolein, dibenzyl, formaldehyde, ethylbenzene, methylstyrene, methylethylbenzene, naphthalene and 4,4' dimethyl-bibenzyl. Only trace amounts of *o*-xylene, indene, methyl-naphthalene, anthracene, phenantrene,

phenyl-acetylene, ethyl benzaldehyde, methyl-biphenyl, diphenyl-butane were detected but not shown here.

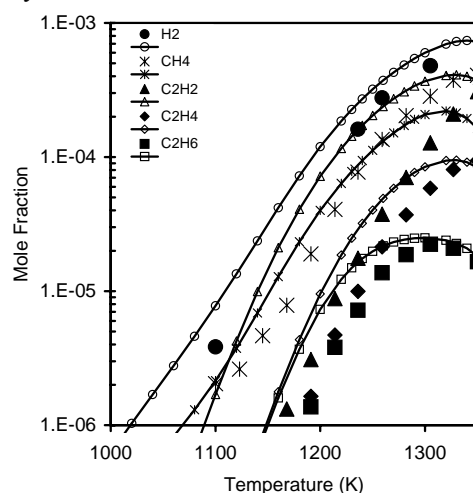


Fig. 3. *M*-xylene oxidation in a JSR at 1 atm. Experimental data (symbols) for hydrogen, methane, acetylene, ethylene and ethane are compared to computations

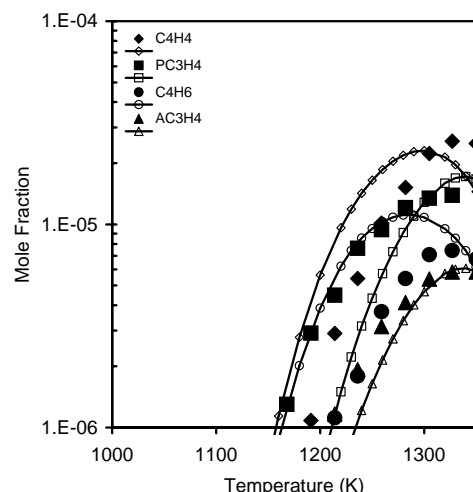


Fig. 4. *M*-xylene oxidation in a JSR at 1 atm. Experimental data (symbols) for vinylacetylene ( $\text{C}_4\text{H}_4$ ), allene ( $\text{AC}_3\text{H}_4$ ), propyne ( $\text{PC}_3\text{H}_4$ ) and 1,3-butadiene ( $\text{C}_4\text{H}_6$ ) are compared to computations

As can be seen from these figures, overall the model represents fairly well the experimental data. The initial conditions were: *p*-xylene, 0.1%;  $\text{O}_2$ , 1.05%,  $\text{N}_2$ , 98.85%,  $\tau=0.1\text{s}$ ;  $\phi=1.0$ . The reactivity of *p*-xylene and the formation of  $\text{CO}$ ,  $\text{CO}_2$ , toluene, benzene, methane, formaldehyde and ethane are well predicted by the model. However, the model strongly over-predicts the formation of acetylene, vinylacetylene, and propyne. Sensitivity analyses and reaction path analyses, based on species reaction rate of production and rate of consumption computations, have also been used to elaborate the presently proposed mechanism and interpret the results for *p*-xylene.

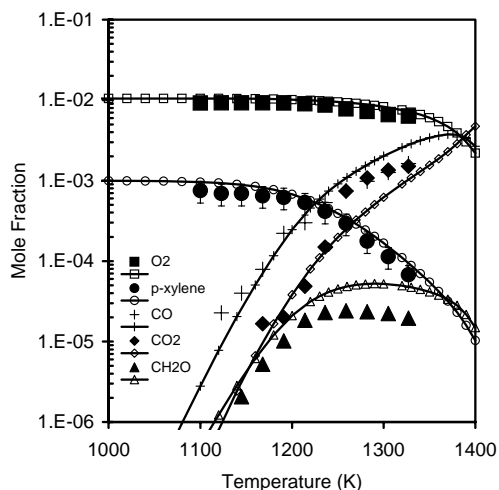


Fig. 5. *P*-xylene oxidation in a JSR at 1 atm. Experimental data (symbols) for CO, formaldehyde ( $\text{CH}_2\text{O}$ ), oxygen and *p*-xylene are compared to computations

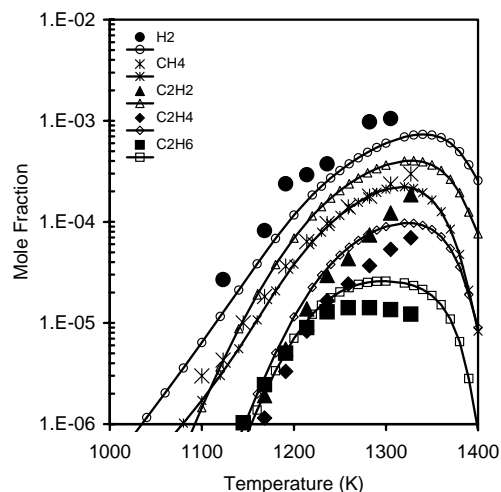


Fig. 7. *P*-xylene oxidation in a JSR at 1 atm. Experimental data (symbols) for hydrogen, methane, acetylene, ethylene and ethane are compared to computations

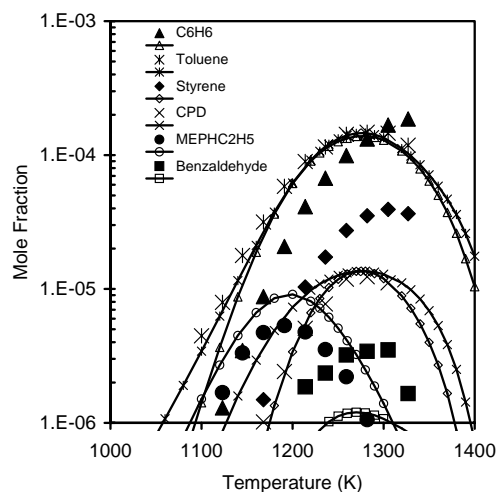


Fig. 6. *P*-xylene oxidation in a JSR at 1 atm. Experimental data (symbols) for benzene ( $\text{C}_6\text{H}_6$ ), toluene, styrene, cyclo-pentadiene (CPD), *p*-methyl-ethylbenzene (MEPHC2H5), benzaldehyde are compared to computations.

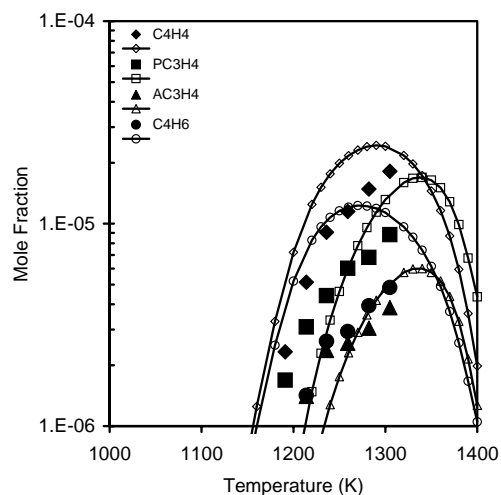
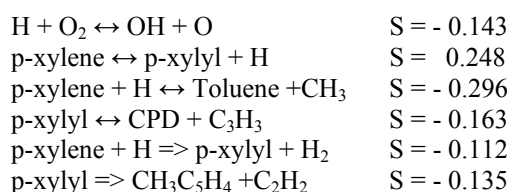


Fig. 8. *P*-xylene oxidation in a JSR at 1 atm. Experimental data (symbols) for vinylacetylene ( $\text{C}_4\text{H}_4$ ), allene ( $\text{AC}_3\text{H}_4$ ), propyne ( $\text{PC}_3\text{H}_4$ ) and 1,3-butadiene ( $\text{C}_4\text{H}_6$ ) are compared to computations

Sensitivity analyses and reaction path analyses, based on species reaction rate of production and rate of consumption computations, were also used to elaborate the presently proposed mechanism and interpret the results for *p*-xylene.

At 1300K, in stoichiometric conditions and at 1 atm, *p*-xylene computed mole fraction is mostly sensitive to:



## Conclusions

For the first time, the oxidation of *m*- and *p*-xylene was studied in a JSR over the temperature range 1050-1400 K, for equivalence ratios of 0.5 to 1.5 and at atmospheric pressure. Molecular species concentration profiles were obtained for 30 species by probe sampling and GC analyses. The JSR experiments were modeled using a detailed chemical kinetic reaction mechanism that was also validated for the oxidation of benzene and toluene over a wide range of conditions. Overall, the proposed kinetic model represents well the experimental results. Kinetic modeling was used to delineate the main reactions involved in the oxidation of *m*- and *p*-xylene. Further kinetic modeling validations are still necessary to cover flame conditions. They would require new experimental data unavailable at the present time: flame speeds and flame structures.

## Acknowledgements

S.G. thanks the French MENRT for a Doctoral grant. The authors are grateful to Dr. F. Lecomte for his help with the experiments and to Dr. M. Cathonnet for his interest in this research.

## References

- [1] J.C. Guibet, Fuels and Engines, Ed. Technip, Paris, 1999.
- [2] J.M. Simmie, Prog. Energ. Comb. Sci., 29 (2003) 599-634.
- [3] P. Dagaut, M. Reuillon, J.C. Boettner, M. Cathonnet, Proc. Combust. Inst. 25 (1994) 919.
- [4] M. Cathonnet, D. Voisin, A. Etsouli, C. Sferdean, M. Reuillon, J.C. Boettner, P. Dagaut, Res. Technol. Org. Meeting Proc. 14 (1999) 14.
- [5] P. Dagaut, Phys. Chem. Chem. Phys. 4 (2002) 2079-2094.
- [6] A. Ristori, P. Dagaut, G. Pengloan, A. El Bakali, M. Cathonnet, Combustion, 1 (2001) 256-294
- [7] P. Dagaut, G. Pengloan, A. Ristori, Phys. Chem. Chem. Phys. 4 (2002) 1846-1854
- [8] P. Dagaut, A. Ristori, A. El Bakali, M. Cathonnet, Fuel 81 (2002) 173-184
- [9] J.L. Emdee, K. Brezinsky, I. Glassman J. Phys. Chem. 95 (1991) 1626
- [10] D. Gregory, R.A. Jackson, Combust. Flame 118 (1999) 459
- [11] A. Roubaud, R. Minetti, L.R. Sochet, Combust. Flame 121 (2000) 535
- [12] L. Dupont, Thesis, Lille, 2001 in French.
- [13] P. Dagaut, M. Cathonnet, J.P. Rouan, R. Foulatier, A. Quilgars, J.C. Boettner, F. Gaillard, H. James, J. Phys. E: Sci Instrum 19 (1986) 207.
- [14] A. El Bakali, M. Braun-Unkloff, P. Dagaut, P. Frank, M. Cathonnet, Proc. Combust. Inst. 28 (2000) 1631-1638.
- [15] P. Glarborg, R.J. Kee, J.F. Grcar, J.A. Miller, Sandia National Laboratories, Livermore, CA, Report No. SAND86-8209, 1986.
- [16] P. Dagaut, F. Lecomte, S. Chevailler, M. Cathonnet, Combust. Sci. Tech. 139 (1998) 329.
- [17] P. Dagaut, J. Luche, M. Cathonnet, Proc. Combust. Inst. 28 (2000) 2459-2465.
- [18] P. Dagaut, M. Cathonnet, Combust. Flame 113 (1998) 620.
- [19] P. Dagaut, M. Cathonnet, Combust. Sci. Tech. 137 (1998) 237.
- [20] P. Dagaut, M. Cathonnet, Combust. Sci. Tech. 140 (1999) 225.
- [21] R.J. Kee, F.M. Rupley, J.A. Miller, Thermodynamic data base, Sandia National Laboratories, Livermore, CA, Report No. SAND87-8215, 1991.
- [22] Y. Tan, P. Dagaut, M. Cathonnet, J.C. Boettner, Combust. Sci. Tech. 102 (1994) 21.
- [23] C. Muller, V. Michel, G. Scacchi, G.M. Côme, J. Chim. Phys. Phys. Chim. Biol. 92 (1995) 1154
- [24] L. Catoire, M.T. Swihart, S. Gail, P. Dagaut, Int. J. Chem. Kinet., 35 (2003) 453-463.
- [25] A.M. Dean, J. Phys. Chem. 89 (1985) 4600.
- [26] D.L. Baulch, C.J. Cobos, R.A. Cox, P. Frank, G. Hayman, Th. Just, J.A. Kerr, T. Murrells, M.J. Pilling, J. Troe, R.W. Walker, J. Warnatz, J. Phys. Chem. Ref. Data 23 (1994) 847.
- [27] W. Müller-Markgraf, J. Troe, J. Phys. Chem. 92 (1988) 4899.